Theoretical Study of the Reactivities of Neutral Six-Membered Carbene Analogues of the Group 13 Elements

Chi-Hui Chen, Meng-Lin Tsai, and Ming-Der Su*

Department of Applied Chemistry, National Chiayi University, Chiayi 60004, Taiwan, Republic of China

Received January 2, 2006

The potential energy surfaces for the chemical reactions of group 13 carbenoids have been studied using density functional theory (B3LYP/LANL2DZ). Five six-membered group 13 carbenoid species, $HC(CMeNPh)_2X$, where X = B, Al, Ga, In, and Tl, have been chosen as model reactants in this work. Also, three kinds of chemical reaction, C−H bond insertion, alkene cycloaddition, and dimerization, have been used to study the chemical reactivities of these group 13 carbenoids. The present theoretical investigations suggest that the relative carbenoidic reactivity decreases in the order B > Al ≫ Ga > In > Tl. That is, the heavier the group 13 atom (X), the more stable is its carbenoid toward chemical reactions. This may be the reason that so far no experimental evidence for the $HC(CMeNPh)_2B$ species has been reported, while the other group 13 carbenoids are isolable at room temperature, since they are quite inert to chemical reaction. Furthermore, the group 13 carbenoid singlet−triplet energy splitting, as described in the configuration mixing model attributed to the work of Pross and Shaik, can be used as a diagnostic tool to predict their reactivities. The results obtained allow a number of predictions to be made.

I. Introduction

The search for group 13 species that are formally analogous to singlet carbenes has continued to occupy the attention of chemists throughout the past decade.[1] Thanks to the advance of new and sophisticated synthetic methodologies, nowadays several group 13 carbenoid molecules can be stabilized to allow their analysis in the solid state.[2−5] These neutral species all feature a planar six-membered heterocycle with the skeletal atoms of the ligand (NCCCN). See **1**. Although there have been a number of reports concerning the chemical and physical properties of such group 13 carbenoid species,[2−5] to the best of our knowledge, neither experimental nor theoretical work has been devoted to a systematic study of their reactivities.

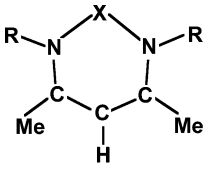

X = Al, Ga, In, Tl
R = Dipp, Trip,.....

1

Our goal in this work is to obtain detailed mechanistic knowledge in order to exercise greater control over their reactions. In fact, a detailed understanding of group 13 carbenoid reactivity is of interest not only for the advancement of basic science but also for the continued development of their applications. Three kinds of chemical reactions are thus discussed in the present work. They are insertion, cycloaddition, and dimerization. These reactions have been chosen because they represent various possible group 13 carbenoid reactions that have already been investigated extensively in the corresponding group 14 systems.[6] We therefore present a density functional theory (DFT) study to investigate the potential energy surfaces and mechanisms of the following reactions:

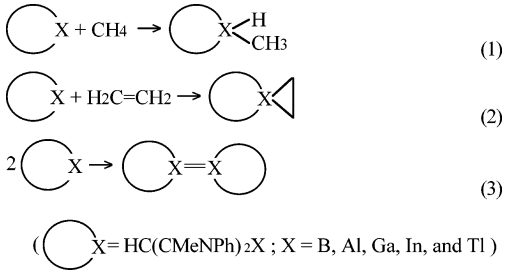

That is, we consider theoretically the reaction paths of three kinds of model reactions involving a series of group 13 carbenoids of the type $HC(CMeNPh)_2X$, where X = B, Al, Ga, In, and Tl. Each of these pathways was examined computationally, and each is described in detail below.

* To whom correspondence should be addressed. E-mail: midesu@mail.ncyu.edu.tw.

(1) For reviews, see: (a) Driess, M.; Grutzmacher, H. *Angew. Chem., Int. Ed.* **1996**, *35*, 829. (b) Power, P. P. *J. Chem. Soc., Dalton Trans.* **1998**, 2939. (c) Power, P. P. *Chem. Rev.* **1999**, *99*, 3463.

(2) The divalent aluminum compounds: (a) Cui, C.; Roesky, H. W.; Schmidt, H.-G.; Noltemeyer, M.; Hao, H.; Cimpoesu, F. *Angew. Chem., Int. Ed.* **2000**, *39*, 4272. (b) Rao, M. N. S.; Roesky, H. W.; Anantharaman, G. *J. Organomet. Chem.* **2002**, *646*, 4.

(3) The divalent gallium compounds: (a) Hardman, N. J.; Eichler, B. E.; Power, P. P. *Chem. Commun.* **2000**, 1991. (b) Hardman, N. J.; Philips, A. D.; Power, P. P. *ACS Symp. Ser.* **2002**, *822*, 2. (c) Schmidt, E. S.; Jockisch, A.; Schmidbaur, H. *J. Am. Chem. Soc.* **1999**, *121*, 9758. (d) Baker, R. J.; Farley, R. D.; Jones, C.; Kloth, M.; Murphy, D. M. *J. Chem. Soc., Dalton Trans.* **2002**, 3844.

(4) The divalent indium compounds: (a) Hill, M. S.; Hitchcock, P. B. *Chem. Commun.* **2004**, 1818. (b) Hill, M. S.; Hitchcock, P. B.; Pongtavornpinyo, R. *J. Chem. Soc., Dalton Trans.* **2005**, 273.

(5) The divalent thallium compounds: (a) Cheng, Y.; Hitchcock, P. B.; Lappert, M. F.; Zhou, M. *Chem. Commun.* **2005**, 752. (b) Ref 4b.

(6) For instance, see: (a) Su, M.-D.; Chu, S.-Y. *Chem. Phys. Lett.* **1999**, *308*, 283. (b) Su, M.−D.; Chu, S.-Y. *Inorg. Chem.* **1999**, *38*, 4819. (c) Su, M.-D.; Chu, S.-Y. *Chem. Phys.* Lett. **2000**, *320*, 475.

10.1021/om0600011 CCC: $33.50
Publication on Web 04/29/2006

Table 1. Selected Geometric Values and Relative Energies for Singlet and Triplet Group 13 Carbenoids, $HC(CMeNPh)_2X$, Where X = B, Al, Ga, In, and Tl[a,b]

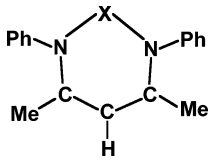

system	X = B	X = Al[c]	X = Ga[d]	X = In[e]	X = Tl[f]
(singlet)					
X−N (Å)	1.451	2.032 [1.957]	2.084 [2.054]	2.256 [2.272]	2.484 [2.416]
N−C (Å)	1.409	1.358 [1.341]	1.356 [1.338]	1.355 [1.323]	1.349 [1.318]
C−C (Å)	1.407	1.413 [1.391]	1.414 [1.400]	1.417 [1.401]	1.421 [1.405]
∠NXN (deg)	116.6	88.71 [89.86]	87.61 [87.53]	83.34 [81.12]	77.32 [76.67]
(triplet)					
X−N (Å)	1.425	1.940	1.954	2.125	2.518
N−C (Å)	1.447	1.352	1.351	1.350	1.392
C−C (Å)	1.404	1.420	1.421	1.422	1.431
∠NXN (deg)	122.6	98.87	97.62	92.68	78.54
ΔE_{st}[g] (kcal mol^{-1})	3.466	45.73	54.46	55.07	54.08

[a] All were calculated at the B3LYP/LANL2DZ (singlet) and UB3LYP/LANL2DZ (triplet) levels of theory. [b] The parameters from experiments are given in brackets. [c] See ref 2a. [d] See ref 3a. [e] See ref 4a. [f] See ref 5a. [g] Energy relative to the corresponding singlet state. A positive value means the singlet is the ground state.

No quantum chemical calculations about these chemical reactions have yet been carried out, let alone a systematic theoretical study undertaken of the effects of element X on the reactivities of group 13 carbenoid species. It is therefore believed that, in view of recent dramatic developments in group 14 heavy-carbene chemistry,[7] analogous extensive studies of group 13 carbenoids should soon be forthcoming and will open up new areas.

II. Theoretical Methods

All geometries were fully optimized without imposing any symmetry constraints, although in some instances the resulting structure showed various elements of symmetry. For our DFT calculations, we used the hybrid gradient-corrected exchange functional proposed by Becke,[8] combined with the gradient-corrected correlation functional of Lee, Yang, and Parr.[9] This functional is commonly known as B3LYP and has been shown to be quite reliable for both geometries and energies.[10] These B3LYP calculations were carried out with relativistic effective core potentials on group 14 elements modeled using the double-ζ (DZ) basis sets[11] augmented by a set of d-type polarization functions.[11e] Accordingly, we denote our B3LYP calculations by B3LYP/LANL2DZ. The spin-unrestricted (UB3LYP) formalism was used for the open-shell (triplet) species. The S^2 expectation values of the triplet state for the reactants all showed an ideal value (2.00) after spin annihilation, so that their geometries and energetics are reliable for this study. Frequency calculations were performed on all structures to confirm that the reactants and products had no imaginary frequencies and that transition states possessed only one imaginary frequency. The relative energies were thus corrected for vibrational zero-point energies (ZPE, not scaled). Thermodynamic corrections to 298 K, ZPE corrections, heat capacity corrections, and entropy corrections (ΔS) obtained were applied at the B3LYP/LANL2DZ level. Thus, the relative free energy (ΔG) at 298 K was also calculated at the same level of theory. All of the DFT calculations were performed using the GAUSSIAN 03 package of programs.[12]

III. Results and Discussion

1. Geometries and Electronic Structures of $HC(CMeNPh)_2X$. Before discussing the geometrical optimizations and the potential energy surfaces for the chemical reactions of the group 13 carbenoids, we shall first examine the geometries and electronic structures of the reactants, i.e., $HC(CMeNPh)_2X$ (X = B, Al, Ga, In, and Tl). The optimized geometries for these group 13 carbenoids were calculated at the B3LYP/LANL2DZ level of theory, and their selected geometrical parameters are collected in Table 1, where they are compared with some available experimental data. Their Cartesian coordinates are included in the Supporting Information.

Reactants $HC(CMeNPh)_2X$ (X = B, Al, Ga, In, and Tl) have been calculated both as singlet and as triplet species. As can be seen in Table 1, the agreement for both bond lengths and bond angles in the rings (X = Al, Ga, In, and Tl) between the B3LYP results and experiments[2−5] for the singlet state is quite good,

(7) For the most recent reviews, see: (a) Weidenbruch, M. *Eur. J. Inorg. Chem.* **1999**, 373. (b) Haaf, M.; Schmedake, T. A.; West, R. *Acc. Chem. Res.* **2000**, *33*, 704. (c) Gehrhus, B.; Lappert, M. F. *J. Organomet. Chem.* **2001**, *617*−*618*, 209. (d) Hill, N. J.; West, R. *J. Organomet. Chem.* **2004**, *689*, 4165. (e) Kira, M. *J. Organomet. Chem.* **2004**, *689*, 4475. (f) Alder, R. W.; Blake, M. E.; Chaker, L. Harvey, J. N.; Paolini, F.; Schutz, J. *Angew. Chem., Int. Ed.* **2004**, *43*, 5896. (g) Refs 1b,c.

(8) (a) Becke, A. D. *Phys. Rev. A* **1988**, *38*, 3098. (b) Becke, A. D. *J. Chem. Phys.* **1993**, *98*, 5648.

(9) Lee, C.; Yang, W.; Parr, R. G. *Phys. Rev. B* **1988**, *37*, 785.

(10) (a) Su, M.-D. *J. Phys. Chem. A* **2004**, *108*, 823. (b) Su, M.-D. *Inorg. Chem.* **2004**, *43*, 4846. (c) Su, M.-D. *Eur. J. Chem.* **2005**, *10*, 5877, and related references therein.

(11) (a) Dunning, T. H., Jr.; Hay, P. J. In *Modern Theoretical Chemistry*; Schaefer, H. F., III, Ed.; Plenum: New York, 1976; pp 1−28. (b) Hay, P. J.; Wadt, W. R. *J. Chem. Phys.* **1985**, *82*, 270. (c) Hay, P. J.; Wadt, W. R. *J. Chem. Phys.* **1985**, *82*, 284. (d) Hay, P. J.; Wadt, W. R. *J. Chem. Phys.* **1985**, *82*, 299. (e) Check, C. E.; Faust, T. O.; Bailey, J. M.; Wright, B. J.; Gilbert, T. M.; Sunderlin, L. S. *J. Phys. Chem. A* **2001**, *105*, 8111.

(12) Frisch, M. J.; Trucks, G. W.; Schlegel, H. B.; Scuseria, G. E.; Robb, M. A.; Cheeseman, J. R.; Zakrzewski, V. G.; Montgomery, J. A., Jr.; Vreven, T.; Kudin, K. N.; Burant, J. C.; Millam, J. M.; Iyengar, S. S.; Tomasi, J.; Barone, V.; Mennucci, B.; Cossi, M.; Scalmani, G.; Rega, N.; Petersson, G. A.; Nakatsuji, H.; Hada, M.; Ehara, M.; Toyota, K.; Fukuda, R.; Hasegawa, J.; Ishida, M.; Nakajima, T.; Honda, Y.; Kitao, O.; Nakai, H.; Klene, M.; Li, X.; Knox, J. E.; Hratchian, H. P.; Cross, J. B.; Adamo, C.; Jaramillo, J.; Gomperts, R.; Stratmann, R. E.; Yazyev, O.; Austin, A. J.; Cammi, R.; Pomelli, C.; Ochterski, J. W.; Ayala, P. Y.; Morokuma, K.; Voth, G. A.; Salvador, P.; Dannenberg, J. J.; Zakrzewski, V. G.; Dapprich, S.; Daniels, A. D.; Strain, M. C.; Farkas, O.; Malick, D. K.; Rabuck, A. D.; Raghavachari, K.; Foresman, J. B.; Ortiz, J. V.; Cui, Q.; Baboul, A. G.; Clifford, S.; Cioslowski, J.; Stefanov, B. B.; Liu, G.; Liashenko, A.; Piskorz, P.; Komaromi, I.; Martin, R. L.; Fox, D. J.; Keith, T.; Al-Laham, M. A.; Peng, C. Y.; Nanayakkara, A.; Challacombe, M.; Gill, P. M. W.; Johnson, B.; Chen, W.; Wong, M. W.; Gonzalez, C.; Pople, J. A. *GAUSSIAN 03*; Gaussian, Inc.: Wallingford, CT, 2003.

with the bond lengths and angles in agreement to within 0.075 Å and 2.2°, respectively. As a result of this encouraging agreement, we believe that the B3LYP calculations will provide an adequate theoretical level for further investigations of molecular geometries, electronic structures, and kinetic features of the reactions.

As expected, no matter what multiplicity the group 13 carbenoids adopt, our computations suggest that the X−N bond distance shows a monotonic increase down the group from B to Tl. The reason for this is mainly due to the increase of atomic radius of X from boron to thallium. Moreover, our theoretical investigations also indicate that, irrespective of its multiplicity, the bond angle ∠NXN decreases uniformly as the central atom, X, is changed from B to Tl. It thus appears that, as the X atom becomes heavier, a more acute bond angle ∠NXN in singlet $HC(CMeNPh)_2X$ is preferred. The reason for this may be due to the relativistic effect.[13] When X changes from boron to thallium, the valence s orbital is more strongly contracted than the corresponding p orbitals.[13] Namely, the size difference between the valence s and p orbitals increases from B to Tl. Consequently, the valence s and p orbitals of the heavier members of the group overlap less to form strong hybrid orbitals.[13] It is therefore expected that a $HC(CMeNPh)_2X$ compound with a heavier X center favors a smaller bond angle ∠NXN.

In the case of cyclic $HC(CMeNPh)_2X$ reactants (X = B, Al, Ga, and In), other interesting trends that can be observed in Table 1 are the decrease in the bond distance X−N and the increase in bond angle ∠NXN on going from the singlet to the triplet state. On the other hand, the triplet state of $HC(CMeNPh)_2Tl$ has a significantly longer bond distance (X−N) and a slightly wider bond angle (∠NXN) than its closed-shell singlet state. The reason for this phenomenon can be understood simply by considering electronic structures (vide infra).

To gain more insight into the nature of chemical bonding in the series of $HC(CMeNPh)_2X$ reactants, the valence molecular orbitals based on the B3LYP/LANL2DZ calculations are presented in Figure 1. The substitution of a single X atom at the $HC(CMeNPh)_2X$ center decreases the energy of the σ orbital on going from B to Tl, i.e., $E\sigma(B) > E\sigma(Al) > E\sigma(Ga) > E\sigma(In) > E\sigma(Tl)$. Likewise, this substitution also decreases the p−π orbital energy down group 13, i.e., $Ep-\pi(B) > Ep-\pi(Al) > Ep-\pi(Ga) > Ep-\pi(In) > Ep-\pi(Tl)$. These two effects lead to a reduced HOMO−LUMO energy difference for the $HC(CMeNPh)_2B$ reactant (vide infra). Note that the nature of the HOMO and the LUMO in $HC(CMeNPh)_2X$, especially for X = Tl, is quite different from that encountered in most group 14 divalent compounds.[14] Here, the HOMO of $HC(CMeNPh)_2X$ (X = B, Al, Ga, and In) is essentially a nonbonding σ orbital. This lone pair orbital is arranged in the cyclic plane of the $HC(CMeNPh)_2X$ species, in a pseudo-trigonal planar fashion with respect to the two sets of X−N linkages. As a result, such lone pairs can be viewed as located within an orbital of predominant sp-character. It is noteworthy that the existence of a nonbonded lone pair of electrons at the X center strongly endorses the singlet carbene character of the group 13 carbenoids (vide infra).

On the other hand, our computations show that, although the HOMO of $HC(CMeNPh)_2X$ (X = B, Al, Ga, and In) corresponds to the X lone pair, their LUMOs do not involve the X p−π orbital. The latter is the LUMO+1 level and separated from the corresponding HOMO by about 74.8 (B), 82.8 (Al), 95.3 (Ga), and 95.9 (In) kcal/mol, respectively. Indeed, previous computational studies on similar model compounds have also concluded that the vacant B, Al, Ga, or In p−π orbital is not the LUMO of these species, but the LUMO+1.[3d,4b] These theoretical studies indicate that the LUMO in each case is entirely ligand-based and of π symmetry, which is consistent with our present work as given in Figure 1. However, our calculations performed upon the singlet $HC(CMeNPh)_2Tl$ species reveal an interesting reordering of the orbital energies. The thallium lone pair (σ) orbital (HOMO−2) is located below its HOMO, which is entirely ligand-based, by about 22 kcal/mol, as demonstrated in Figure 1. This observation may be attributed to the "orbital nonhybridization effect", also known as the "inert s-pair effect", as mentioned earlier.[13] Similarly, the LUMO of $HC(CMeNPh)_2Tl$ corresponds to the thallium p−π orbital, which is about 115 kcal/mol above the corresponding lone pair (σ) orbital (HOMO−2).

Furthermore, the other striking feature is the singlet−triplet splitting ($\Delta E_{st} = E_{triplet} - E_{singlet}$). As one can see in Table 1, our DFT calculations indicate that the singlet−triplet splittings for boron, aluminum, gallium, indium, and thallium are 3.5, 46, 54, 55, and 54 kcal/mol, respectively; that is, ΔE_{st} increases in the order B < Al < Ga ≈ Tl < In. In other words, the singlet−triplet gap for the group 13 $HC(CMeNPh)_2X$ species shows a different order from that of the group 14 carbene species, in which the energy gap usually increases in the order C < Si < Ge < Sn < Pb.[14] Again, as mentioned earlier, the reason for such a difference can be traced directly to electronic factors. From Figure 1, it is apparent that the magnitude of the energy difference between HOMO and LUMO for the cyclic $HC(CMeNPh)_2X$ systems becomes larger as one proceeds along the series from B to Tl. This observation can explain why the $HC(CMeNPh)_2B$ molecule has a quite small singlet−triplet splitting ($\Delta E_{st} = -3.5$ kcal/mol), whereas the other group 13 $HC(CMeNPh)_2X$ species have comparatively large singlet−triplet separations ($\Delta E_{st} > 45$ kcal/mol). In fact, the stabilities of the carbene analogues are determined by the singlet−triplet energy separations in $HC(CMeNPh)_2X$. If ΔE_{st} is small, the carbene-type structures will not be stable and will be capable of facile chemical reactions (such as with solvents, etc.). Accordingly, the small singlet−triplet energy splitting in the boron case strongly implies that this species is too unstable to be detected experimentally. The supporting evidence comes from the fact that so far the boron carbenoid species with a six-membered ring has not been experimentally identified and separated.[2−5]

Finally, as seen from Table 1, our DFT calculations indicate that the $HC(CMeNPh)_2X$ (X = B, Al, Ga, In, and Tl) species all possess a singlet ground state. This strongly indicates that all three reactions (eqs 1−3) should proceed on the singlet surface. We shall thus focus on the singlet surface from now on.

2. Geometries and Energetics of $HC(CMeNPh)_2X + CH_4$. Next, let us consider mechanisms that proceed via eq 1, focusing on the transition states as well as on the insertion products themselves. That is, the insertion mechanisms may be thought to proceed as follows: reactants (**Rea-CH_4**) → transition state (**TS-CH_4**) → products (**Pro-CH_4**). The optimized geometries calculated at the B3LYP/LANL2DZ level of theory involving **Rea-CH_4**, **TS-CH_4**, and **Pro-CH_4** are collected in Figure 2. To simplify the comparisons and to emphasize the trends, we have also given the energies relative to the two reactant molecules, i.e., $HC(CMeNPh)_2X + CH_4$, which are summarized in Table

(13) (a) Pykkö, P.; Desclaux, J.-P. *Acc. Chem. Res.* **1979**, *12*, 276. (b) Kutzelnigg, W. *Angew. Chem., Int. Ed. Engl.* **1984**, *23*, 272. (c) Pykkö, P. *Chem. Rev.* **1988**, *88*, 563. (d) Pyykkö, P. *Chem. Rev.* **1997**, *97*, 597.

(14) (a) Su, M.-D.; Chu, S.-Y. *Inorg. Chem.* **1999**, *38*, 4819. (b) Su, M.-D. *J. Phys. Chem. A* **2002**, *106*, 9563.

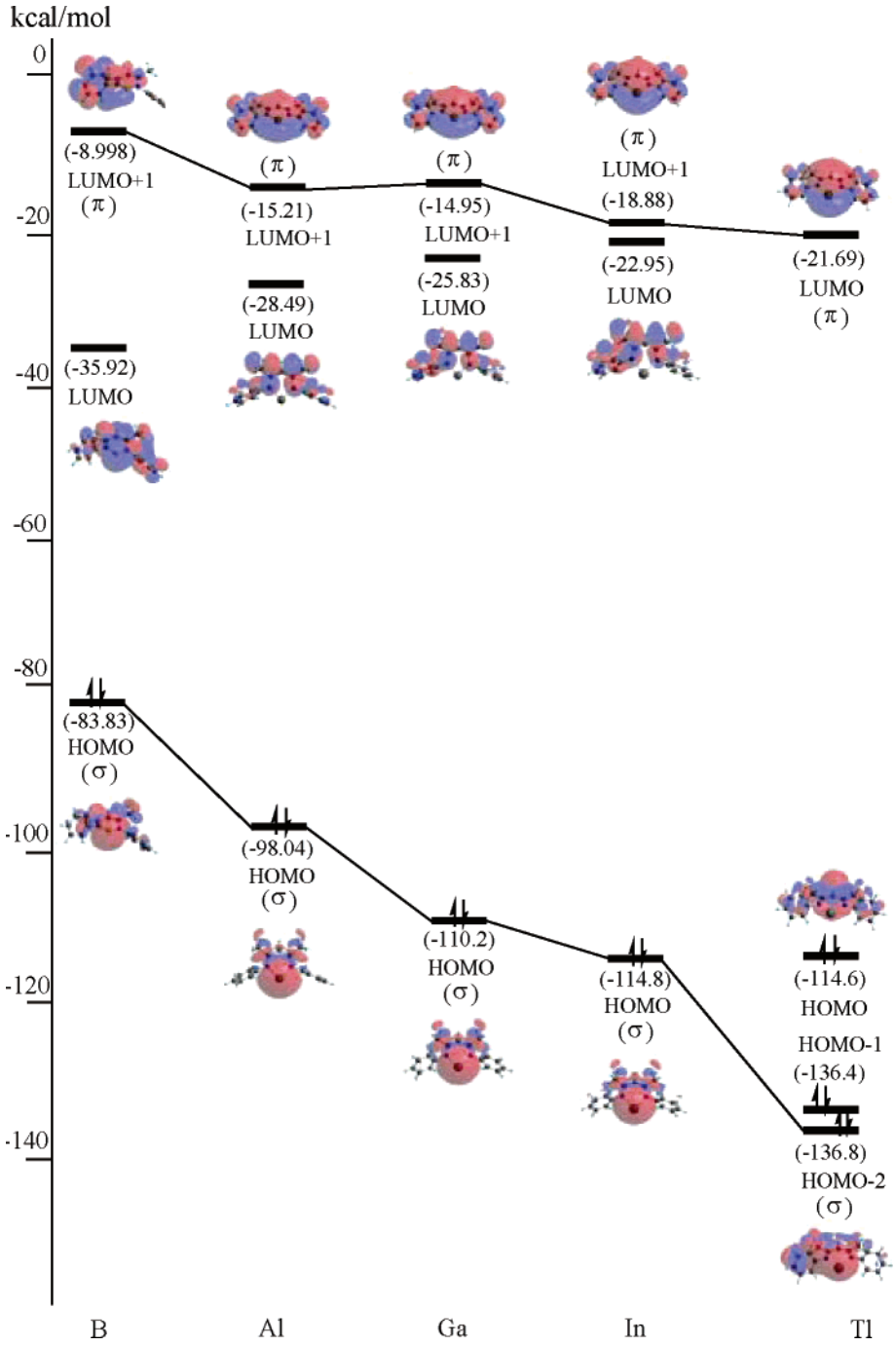

Figure 1. Calculated frontier molecular orbital for the $HC(CMeNPh)_2X$ (X = B, Al, Ga, In, and Tl) species. For more information see the text.

2. Cartesian coordinates calculated for the stationary points at the B3LYP level are available as Supporting Information. There are several important conclusions from these results to which attention should be drawn.

(1) Considering the C−H bond insertion reaction path, we have located the transition state for each $HC(CMeNPh)_2X$ case (**TS-CH_4-B**, **TS-CH_4-Al**, **TS-CH_4-Ga**, **TS-CH_4-In**, and **TS-CH_4-Tl**) at the B3LYP/LANL2DZ level of theory. The optimized geometries of the five transition states can be found in Figure 2. All five transition state structures show the same three-center pattern involving X (X = B, Al, Ga, In, and Tl), carbon, and hydrogen atoms. The transition state vectors are in accordance with an insertion process, primarily with C−H bond stretching accompanied by a hydrogen atom migrating to the X center. The B3LYP eigenvalues give an imaginary frequency (cm^{-1}) of 995i (**TS-CH_4-B**), 1205i (**TS-CH_4-Al**), 1160i (**TS-CH_4-Ga**), 1097i (**TS-CH_4-In**), and 1113i (**TS-CH_4-Tl**). As seen in Figure 2, in the transition state, there is a trend as X increases in atomic weight for the stretching C−H bond to become longer and for the forming X−H bond length to increase relative to that in the final product. For instance, the breaking C−H bond lengths (Å) are 1.600 (B), 1.749 (Al), 1.821 (Ga), 1.931 (In), and 2.222 (Tl), respectively. These values suggest that the C−H bond insertion takes place earlier along the reaction coordinate. Thus, the X−H and X−C bond lengths in the transition structure are more product-like for X = In and Tl and more reactant-like for X = B. According to the Hammond postulate,[15] **TS-CH_4-In** and **TS-CH_4-Tl** should have the highest and **TS-CH_4-B** the

(15) Hammond, G. S. *J. Am. Chem. Soc.* **1954**, *77*, 334.

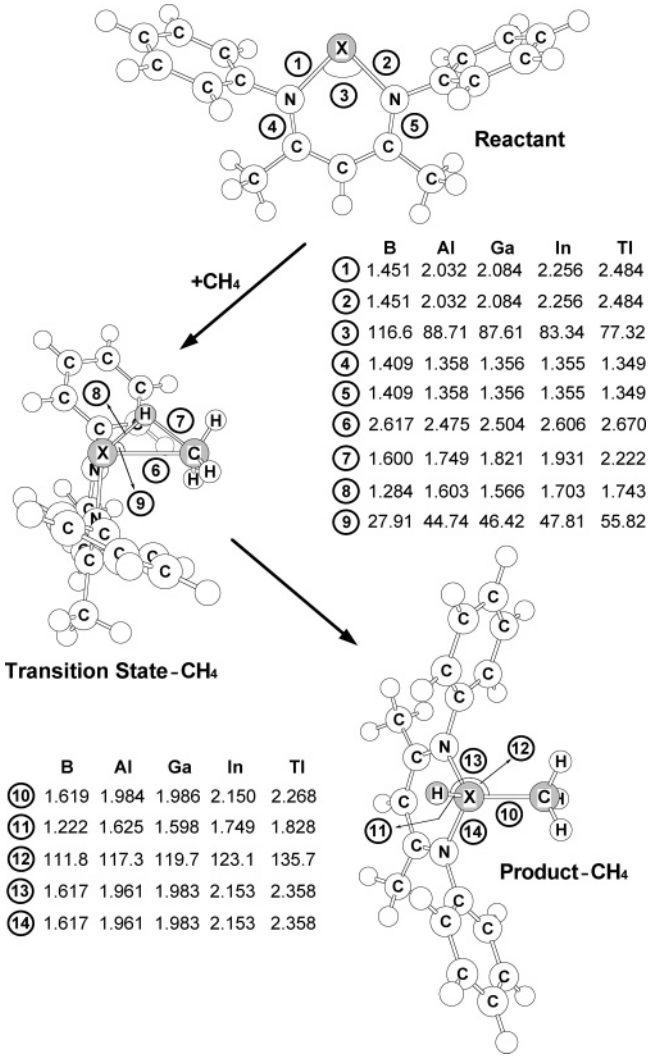

	B	Al	Ga	In	Tl
①	1.451	2.032	2.084	2.256	2.484
②	1.451	2.032	2.084	2.256	2.484
③	116.6	88.71	87.61	83.34	77.32
④	1.409	1.358	1.356	1.355	1.349
⑤	1.409	1.358	1.356	1.355	1.349
⑥	2.617	2.475	2.504	2.606	2.670
⑦	1.600	1.749	1.821	1.931	2.222
⑧	1.284	1.603	1.566	1.703	1.743
⑨	27.91	44.74	46.42	47.81	55.82

	B	Al	Ga	In	Tl
⑩	1.619	1.984	1.986	2.150	2.268
⑪	1.222	1.625	1.598	1.749	1.828
⑫	111.8	117.3	119.7	123.1	135.7
⑬	1.617	1.961	1.983	2.153	2.358
⑭	1.617	1.961	1.983	2.153	2.358

Figure 2. B3LYP/LANL2DZ-optimized geometries (in Å and deg) of the reactants (singlet), transition states, and insertion products of $HC(CMeNPh)_2X$ (X = B, Al, Ga, In, and Tl) and CH_4. For relative energies for each species, see Table 2. Hydrogens are omitted for clarity.

smallest activation barriers. This was fully confirmed by our theoretical calculations. As shown in Table 2, the barrier height for the C−H insertion reaction increases in the order (kcal/mol) **TS-CH$_4$-B** (+20) < **TS-CH$_4$-Al** (+52) < **TS-CH$_4$-Ga** (+59) < **TS-CH$_4$-In** (+70) < **TS-CH$_4$-Tl** (+105). In other words, the greater the atomic number of the X center, the greater the C−H insertion barrier.

(2) On the other hand, the optimized product structures (**Pro-CH$_4$-B**, **Pro-CH$_4$-Al**, **Pro-CH$_4$-Ga**, **Pro-CH$_4$-In**, and **Pro-CH$_4$-Tl**) are collected in Figure 2, and the calculated reaction enthalpies for insertion are given in Table 2. Again, as Figure 2 shows, the order of the X−C bond length follows the same trend as the atomic weight of the central atom X: **Pro-CH$_4$-B** (1.62 Å) < **Pro-CH$_4$-Al** (1.98 Å) < **Pro-CH$_4$-Ga** (1.99 Å) < **Pro-CH$_4$-In** (2.15 Å) < **Pro-CH$_4$-Tl** (2.27 Å). To our knowledge, experimental structures for such compounds are not known as yet.[2−5] As mentioned above, a group 13 carbenoid with a less massive but more electronegative central atom reaches the transition state relatively early, whereas one with a more massive and less electronegative central atom arrives relatively late. The former is therefore predicted to undergo a more exothermic insertion, which is borne out by our B3LYP calculations. For instance, the order of exothermicity follows the same trend as

Table 2. Relative Energies for Singlet and Triplet Group 13 Carbenoids ($HC(CMeNPh)_2X$) and for the CH_4 Insertion Process: Reactants ($HC(CMeNPh)_2X + CH_4$) → Transition State → Insertion Product[a,b]

system	ΔE_{st}[3] (kcal mol^{-1})	$\Delta E^{\ddagger}$[d] (kcal mol^{-1})	ΔH[e] (kcal mol^{-1})
X = B	3.466	20.09	−50.48
X = Al	45.73	52.26	−22.57
X = Ga	54.46	59.35	−11.66
X = In	55.07	69.50	4.116
X = Tl	54.08	105.2	48.87

[a] All were calculated at the B3LYP/LANL2DZ level of theory. For the B3LYP-optimized structures of the stationary points, see Figure 2. [b] Energy differences have been zero-point corrected. See the text. [c] Energy relative to the corresponding singlet state. A positive value means the singlet is the ground state. [d] The activation energy of the transition state, relative to the corresponding reactants. [e] The reaction enthalpy of the product, relative to the corresponding reactants.

the activation energy (kcal/mol): **Pro-CH$_4$-B** (−50) < **Pro-CH$_4$-Al** (−23) < **Pro-CH$_4$-Ga** (−12) < **Pro-CH$_4$-In** (+4.1) < **Pro-CH$_4$-Tl** (+49). Note that the energies of **Pro-CH$_4$-In** and **Pro-CH$_4$-Tl** are above those of their corresponding starting materials. This strongly implies that CH_4 insertion by $HC(CMeNPh)_2In$ and $HC(CMeNPh)_2Tl$ are energetically unfavorable and would be endothermic. Namely, our theoretical findings suggest that the insertion products of indium and thallium carbenoids should not be produced from the C−H bond insertion reaction of $HC(CMeNPh)_2In + CH_4 \rightarrow HC(CMeNPh)_2In(H)(CH_3)$ and $HC(CMeNPh)_2Tl + CH_4 \rightarrow HC(CMeNPh)_2Tl(H)(CH_3)$, respectively, but possibly exist if these two final products are produced through other reaction paths.

(3) All the above DFT results can be rationalized on the basis of a configuration mixing (CM) model attributed to the work of Pross and Shaik.[16,17] According to this model, the stabilization of an insertion TS depends on the singlet−triplet splitting ΔE_{st} ($= E_{triplet} - E_{singlet}$) of the reactant group 13 carbenoid; that is, a smaller ΔE_{st} results in a greater TS stabilization, a lower activation energy, a faster insertion reaction, and a greater exothermicity. Before further discussion, let us emphasize here the importance of the status of the triplet state for the group 13 carbenoid reactant. Since two new covalent bonds have to be formed in the insertion product $HC(CMeNPh)_2X(H)(CH_3)$, i.e., the X−H and X−C bonds (Figure 2), the bond-prepared $HC(CMeNPh)_2X$ state thus has to have at least two open shells, and the lowest state of this type is the triplet state. Therefore, from the valence-bond point of view,[16,17] the bonding in the product can be recognized as bonds formed between the triplet $HC(CMeNPh)_2X$ state and the two doublet radicals (overall singlet), the methyl radical, and the hydrogen atom. This is much in the same way as the bonding in the water molecule can be considered as bonds formed between the triplet oxygen atom and the two doublet hydrogen atoms.[18] Accordingly, if a reactant $HC(CMeNPh)_2X$ has a singlet ground state with a small excitation energy to the triplet state, this will bring more opportunities for the triplet state to take part in the singlet

(16) For details, see: (a) Shaik, S.; Schlegel, H. B.; Wolfe, S. In *Theoretical Aspects of Physical Organic Chemistry*; John Wiley & Sons Inc.: New York, 1992. (b) Pross, A. In *Theoretical and Physical Principles of Organic Reactivity*; John Wiley & Sons Inc.: New York, 1995. (c) Shaik, S. *Prog. Phys. Org. Chem.* **1985**, *15*, 197. (d) Shaik, S. In *Theory and Applications of Computational Chemistry*; Dykstra, C. E., Frenking, G., Kim, K. S., Scuseria, G. E., Eds.; Elsevier: New York, 2003.

(17) (a) For the first paper that originated the CM model see: Shaik, S. *J. Am. Chem. Soc.* **1981**, *103*, 3692. (b) About the most updated review of the CM model: Shaik, S.; Shurki, A. *Angew. Chem., Int. Ed.* **1999**, *38*, 586.

(18) Su, M.-D. *Chem. Eur. J.* **2004**, *10*, 5877.

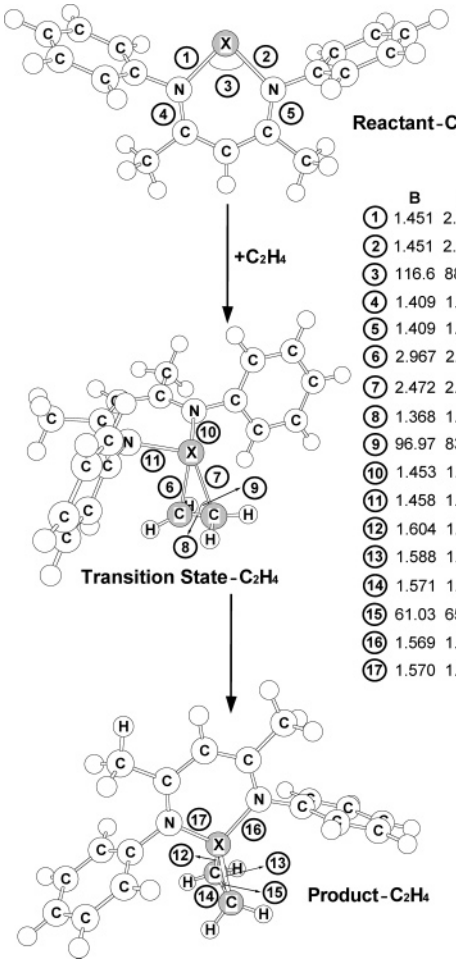

	B	Al	Ga	In	Tl
1	1.451	2.032	2.084	2.256	2.484
2	1.451	2.032	2.084	2.256	2.484
3	116.6	88.71	87.61	83.34	77.32
4	1.409	1.358	1.356	1.355	1.349
5	1.409	1.358	1.356	1.355	1.349
6	2.967	2.385	2.336	2.338	2.309
7	2.472	2.066	2.028	2.161	2.239
8	1.368	1.454	1.471	1.502	1.610
9	96.97	83.34	82.08	77.01	71.62
10	1.453	1.943	1.953	2.116	2.299
11	1.458	1.949	1.962	2.116	2.292
12	1.604	1.954	1.966	2.136	2.268
13	1.588	1.949	1.959	2.125	2.258
14	1.571	1.621	1.613	1.603	1.623
15	61.03	65.64	65.95	68.25	69.32
16	1.569	1.925	1.942	2.112	2.300
17	1.570	1.925	1.941	2.111	2.298

Figure 3. B3LYP/LANL2DZ-optimized geometries (in Å and deg) of the reactants (singlet), transition states, and addition products of $HC(CMeNPh)_2X$ (X = B, Al, Ga, In, and Tl) and C_2H_4. For relative energies for each species, see Table 3. Hydrogens are omitted for clarity.

reaction and a single-step bond insertion is expected to take place more readily. As discussed earlier, our DFT results suggest an increasing trend in ΔE_{st} for the $HC(CMeNPh)_2X$ reactant as follows: B (3.5 kcal/mol) < Al (46 kcal/mol) < Ga (54 kcal/mol) ≈ Tl (54 kcal/mol) < In (55 kcal/mol). This result is in accordance with the trend in activation energy and reaction enthalpy ($\Delta E^{\ddagger}$, ΔH) for group 13 carbenoid species, which are (20, −50), (52, −23), (59, −12), (70, +4.1), and (105, +49) kcal/mol. These results strongly support the predictions as mentioned previously: *the smaller the ΔE_{st} of the group 13 carbenoid, $HC(CMeNPh)_2X$, the lower the barrier height and, in turn, the faster the insertion reaction and the greater the exothermicity*.

3. Geometries and Energetics of $HC(CMeNPh)_2X + C_2H_4$. We now consider the cycloaddition reactions of the group 13 carbenoids $HC(CMeNPh)_2X$ with π-type species, such as ethylene. For consistency with our earlier work, the following reaction mechanism has been used to explore the cycloaddition reaction of $HC(CMeNPh)_2X$ to ethylene: reactants (**Rea-C_2H_4**) → transition state (**TS-C_2H_4**) → cycloaddition products (**Pro-C_2H_4**). Selected geometrical parameters of these critical points along the cycloaddition reaction path are collected in Figure 3. Also, their relative B3LYP/LANL2DZ energies are summarized in Table 3. Their Cartesian coordinates are given in the Supporting Information. Several noteworthy features from Figure 3 and Table 3 are revealed.

Table 3. Relative Energies for Singlet and Triplet Group 13 Carbenoids ($HC(CMeNPh)_2X$) and for the C_2H_4 Addition Process: Reactants ($HC(CMeNPh)_2X + C_2H_4$) → Transition State → Addition Product[a,b]

system	ΔE_{st}[c] (kcal mol^{-1})	$\Delta E^{\ddagger}$[d] (kcal mol^{-1})	ΔH[e] (kcal mol^{-1})
X = B	3.466	1.844	−51.98
X = Al	45.73	12.28	−8.937
X = Ga	54.46	20.13	6.487
X = In	55.07	31.42	26.81
X = Tl	54.08	78.28	78.32

[a] All were calculated at the B3LYP/LANL2DZ level of theory. For the B3LYP-optimized structures of the stationary points, see Figure 3. [b] Energy differences have been zero-point corrected. See the text. [c] Energy relative to the corresponding singlet state. A positive value means the singlet is the ground state. [d] The activation energy of the transition state, relative to the corresponding reactants. [e] The reaction enthalpy of the product, relative to the corresponding reactants.

(1) Since the vast majority of theoretical studies have been devoted to the analysis of the addition reactions of singlet carbene,[19,20] we shall apply the same theoretical model to the group 13 carbenoid systems. The addition of a singlet $HC(CMeNPh)_2X$ to an ethylene involves simultaneous interactions between the vacant carbenoid p orbital (the π orbital; see Figure 1) and the filled ethylene π orbital (HOMO) and between the filled carbenoid σ orbital (HOMO; see Figure 1) and the vacant ethylene π^* orbital (LUMO). Although a singlet $HC(CMeNPh)_2X$ is inherently both an electrophile and a nucleophile, its behavior here is determined by the electron distribution in the transition state. This, in turn, depends on whether the $\pi_{carbenoid}/HOMO_{ethylene}$ or $\sigma_{carbenoid}/LUMO_{ethylene}$ interaction is stronger in this state. Moreover, according to Hoffmann's work,[19a] there are two possible routes of approach of a $HC(CMeNPh)_2X$ to an olefin as shown in **2** and **3**. The π approach (**2**) (nonleast motion), with the p orbital of $HC(CMeNPh)_2X$ impinging on the π system of the alkene, has only one plane of symmetry, making this reaction symmetry-allowed. On the other hand, **3** gives the most symmetrical transition state and has been called σ approach (least motion) because the σ orbital of the $HC(CMeNPh)_2X$ impinges on the ethylene π system. Hoffmann has pointed out that the σ approach (**3**) is "forbidden" in terms of the conservation of orbital symmetry and is therefore expected to be high in energy.[19] On this basis, the preferred approach should be the π approach (**2**), in which the filled π molecular orbital interacts with the empty p orbital of the group 13 carbenoid. Our DFT calculations support this prediction, as will be shown below.

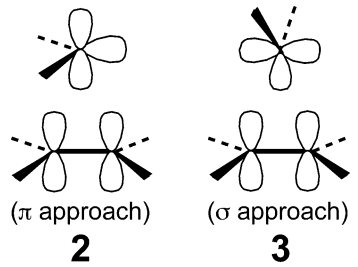

(2) We have located the transition state for each group 13 carbenoid species (**TS-C_2H_4-B**, **TS-C_2H_4-Al**, **TS-C_2H_4-Ga**, **TS-C_2H_4-In**, and **TS-C_2H_4-Tl**) at the B3LYP/LANL2DZ level of

(19) (a) Hoffmann, R. *J. Am. Chem. Soc.* **1968**, *90*, 1475. (b) Zurawski, B.; Kutzelnigg, W. *J. Am. Chem. Soc.* **1978**, *100*, 2654. (c) Rondan, N. G.; Houk, K. N.; Moss, R. A. *J. Am. Chem. Soc.* **1980**, *102*, 1770.

(20) Su, M.-D, *J. Phys. Chem.* **1996**, *100*, 4339, and related references therein.

theory as shown in Figure 3. Our DFT calculations indicate that the main component of the transition vector corresponds to the displacement of $HC(CMeNPh)_2X$ toward the ethylene, whose eigenvalue gives an imaginary frequency of 193i (**TS-C_2H_4-B**), 294i (**TS-C_2H_4-Al**), 260i (**TS-C_2H_4-Ga**), 180i (**TS-C_2H_4-In**), and 46i cm^{-1} (**TS-C_2H_4-Tl**). Moreover, the transition states of all the reactions investigated have a common structure, in which $HC(CMeNPh)_2X$ is slightly off-center. From Figure 3, it is readily seen that, in all of the TS structures, the group 13 X atom in $HC(CMeNPh)_2X$ is initially bonded to only one of the carbon atoms in ethylene, i.e., $X-C_1 \neq X-C_2$. This means that the mechanism of the singlet $HC(CMeNPh)_2X$ addition to ethylene is the asynchronous one. A similar asynchronous approach had previously been found for the addition to ethylene in free methylene.[19] In addition, the B3LYP calculations demonstrate that all the TSs studied in this work have a parallel plane approach of $HC(CMeNPh)_2X$ to ethylene in the formation of the π-TS, as shown in Figure 3. This suggests that the singlet $HC(CMeNPh)_2X$ species exhibit electrophilic character in the addition reactions with an alkene and that the internal pathway in the mutual approach of the reactants is predominantly a π approach. Thus, our calculations support the predictions, as mentioned earlier, that the group 13 carbenoid avoids forbiddenness by a π approach, rather than by a σ approach.

(3) The activation barriers for the cycloaddition reactions are presented in Table 3. The energy of the transition state relative to its corresponding reactants is predicted to be in the order (kcal/mol) **TS-C_2H_4-B** (+1.8) < **TS-C_2H_4-Al** (+12) < **TS-C_2H_4-Ga** (+20) < **TS-C_2H_4-In** (+31) < **TS-C_2H_4-Tl** (+78). The expected products of the cycloaddition reactions of $HC(CMeNPh)_2X$ with ethylene are three-membered rings, heavier analogues of cyclopropane. Experimental structures for these cyclic compounds are not to our knowledge known. Our theoretical calculations suggest that the trend in reaction enthalpy (kcal/mol) also mirrors the trend in activation energy: **Pro-C_2H_4-B** (−52) < **Pro-C_2H_4-Al** (−8.9) < **Pro-C_2H_4-Ga** (+6.5) < **Pro-C_2H_4-In** (+27) < **Pro-C_2H_4-Tl** (+78). Again, these trends reflect that of ΔE_{st}, which increases as X changes from B down to Tl. These results are also consistent with the prediction based on the CM model that the activation barrier should be correlated with the reaction enthalpy for a cycloaddition.[16,17] Finally, it should be noted that the energies of the cycloaddition products for the gallium, indium, and thallium systems are above those of the corresponding reactants. This strongly implies that the cycloaddition reactions of gallium, indium, and thallium carbenoids to alkenes should be energetically unfavorable from both kinetic and thermodynamic viewpoints.

4. Geometries and Electronic Structures of Dimerization Reactions. To obtain further information about the kinetic stability of $HC(CMeNPh)_2X$, one possible chemical reaction was investigated: the propensity for dimerization. Selected geometrical parameters for the stationary point structures along the pathway given in eq 3 and calculated at the B3LYP/LANL2DZ level are shown in Figure 4. The relative energies obtained at the same level of theory are collected in Table 4. Cartesian coordinates for these stationary points are included in the Supporting Information. The major conclusions that can be drawn from the current study are as follows.

(1) During the dimerization, a double-bond formation is assumed between the two rings. Since there are two bulky protecting groups around the group 13 X center (see **1**), the two monomer molecules were thus positioned with the two six-membered ring planes nearly orthogonal to each other. However, repeated attempts to find the transition state for a concerted dimerization of two $HC(CMeNPh)_2X$ species using the DFT methodology failed. Our theoretical investigations therefore suggested that no transition states exist on the B3LYP/LANL2DZ surface for the dimerization of group 13 carbenoids.

(2) Nevertheless, our computational results indicate that all five dimers ($HC(CMeNPh)_2X{=}X(CMeNPh)_2CH$; X = B, Al, Ga, In, and Tl) contain no imaginary frequency and, in turn, can be considered as true minima on the B3LYP potential energy surfaces. Unfortunately, as we have mentioned earlier, because of a lack of experimental and theoretical data on such double-bonded species, the geometrical values presented in this work should be considered as predictions for future investigations. The most noteworthy feature about such dimers is that they do

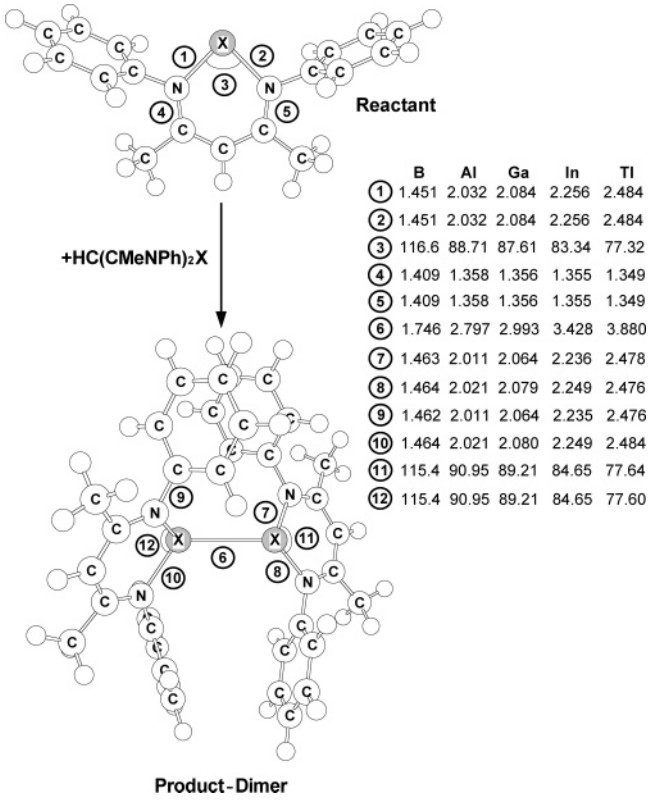

	B	Al	Ga	In	Tl
1	1.451	2.032	2.084	2.256	2.484
2	1.451	2.032	2.084	2.256	2.484
3	116.6	88.71	87.61	83.34	77.32
4	1.409	1.358	1.356	1.355	1.349
5	1.409	1.358	1.356	1.355	1.349
6	1.746	2.797	2.993	3.428	3.880
7	1.463	2.011	2.064	2.236	2.478
8	1.464	2.021	2.079	2.249	2.476
9	1.462	2.011	2.064	2.235	2.476
10	1.464	2.021	2.080	2.249	2.484
11	115.4	90.95	89.21	84.65	77.64
12	115.4	90.95	89.21	84.65	77.60

Figure 4. B3LYP/LANL2DZ-optimized geometries (in Å and deg) of the reactants (singlet) and dimer products of $HC(CMeNPh)_2X$ (X = B, Al, Ga, In, and Tl). For relative energies for each species, see Table 4. Hydrogens are omitted for clarity. For more information, see the text.

Table 4. Relative Energies for Singlet and Triplet Group 13 Carbenoids ($HC(CMeNPh)_2X$) and for the Dimerization Process: Reactants ($2HC(CMeNPh)_2X$) → Dimerization Product

system	ΔE_{st}[c] (kcal mol^{-1})	ΔH[d] (kcal mol^{-1})	ΔG[e] (kcal mol^{-1})
X = B	3.466	−70.62	−54.30
X = Al	45.73	0.4418	14.88
X = Ga	54.46	3.443	18.32
X = In	55.07	2.701	17.62
X = Tl	54.08	0.8992	10.57

[a] All were calculated at the B3LYP/LANL2DZ level of theory. For the B3LYP-optimized structures of the stationary points, see Figure 4. [b] Energy differences have been zero-point corrected. See the text. [c] Energy relative to the corresponding singlet state. A positive value means the singlet is the ground state. [d] The reaction enthalpy of the product, relative to the corresponding reactants. [e] The Gibbs free energy (298 K) of the product, relative to the corresponding reactants.

not exhibit classical planar geometry, but rather have a trans-bent structure (**4**), with pyramidalization of both $HC(CMeNPh)_2X$ groups. Indeed, it is well established that the "trans-bent" compound, containing so-called "nonclassical double bonds", is a minimum on the potential energy surface for all of the heavier analogues of ethylene, from Si_2H_4 to Pb_2H_4.[21] Nevertheless, it should be mentioned that our B3LYP results suggest that the B═B dimer studied in this work adopts a different conformation, a perpendicular structure (**5**).[22] As demonstrated in Figure 4, the trend in X═X bond length in the dimer molecule was calculated to be in the order 1.746 Å (B═B) < 2.797 Å (Al═Al) < 2.993 Å (Ga═Ga) < 3.387 Å (In═In) < 3.580 Å (Tl═Tl), correlating with the atomic size of the main group 13 element X as it changes from B to Tl. In addition, our DFT results suggest that the greater the atomic number of the group 13 element, the greater the pyramidalization angle θ (or out-of-plane angle). For instance, the pyramidalization angle θ increases in the order 52° (Al═Al) < 55° (Ga═Ga) < 59° (In═In) < 63° (Tl═Tl). Again, the pyramidalization angles in In═In and Tl═Tl are far away from 0° (planar) and provide evidence for the core-like nature of the 5s and 6s electrons, that is, for the so-called "inert s-pair effect",[13] discussed earlier. Apparently, the heavier group 13 elements are pivotal atoms in this regard. These results are consistent with those reported in the previous studies cited above and will not be discussed further.

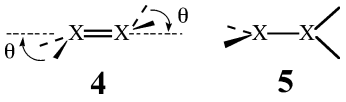

4 **5**

(3) As one can see in Table 4, our B3LYP results demonstrate that the energy of the final products (dimers) relative to their corresponding reactants are −71 (B═B), +0.44 (Al═Al), +3.4 (Ga═Ga), +2.7 (In═In), and +0.90 (Tl═Tl) kcal/mol. Also, we have calculated the free energy differences (ΔG) for eq 3 at 298 K, which are also given in Table 4. As shown there, the values of ΔG (kcal/mol) between reactants and dimer are −54, 15, 18, 18, and 11 for boron, aluminum, gallium, indium, and thallium, respectively. Accordingly, these results predict that boron derivatives having B═B bonded dimeric structures are both kinetically and thermodynamically stable with respect to dissociation. In contrast to the boron compounds, the theoretical results indicate that, after considering the thermodynamic factors, the total energies of the remaining double-bonded dimers are still above that of two separated monomers ($HC(CMeNPh)_2X$). Our theoretical findings therefore strongly suggest that the dimerization reaction should not occur during the formation of the $HC(CMeNPh)_2X$ (X = Al, Ga, In, and Tl) species. Indeed, our theoretical conclusions are in good agreement with the available experimental observations.[2−5]

IV. Conclusion

Taking all three aforementioned reactions studied in this work together, one can draw the following conclusions.

(1) In the case of boron, $HC(CMeNPh)_2B$ can readily undergo concerted C−H bond insertion and cycloaddition by reaction with methane and ethylene, respectively. In particular, our theoretical results find no barrier to the dimerization reaction of $HC(CMeNPh)_2B$. Namely, once the $HC(CMeNPh)_2B$ molecule is formed, dimerization can proceed without any difficulty at room temperature. In consequence, our theoretical findings strongly imply that, compared with the other group 13 carbenoids, the $HC(CMeNPh)_2B$ species should be unstable and cannot be readily synthesized and isolated. Indeed, so far no experimental evidence for $HC(CMeNPh)_2B$ has been reported.[2−5]

(2) In the case of aluminum, gallium, indium, and thallium, on the contrary, the $HC(CMeNPh)_2X$ (X = Al, Ga, In, and Tl) cannot undergo C−H bond insertion, cycloaddition, and dimerization reactions, since they are all energetically unfeasible processes from both a kinetic and thermodynamic viewpoint. From another point of view, our theoretical findings confirm a general belief that one of the important influences on the isolability of a group 13 carbenoid is its group 13 atom center. Indeed, it has been reported that only the $HC(CMeNPh)_2X$ (X = Al, Ga, In, and Tl) species are isolable compounds at room temperature.[2−5]

(3) The reactivity of group 13 carbenoids ($HC(CMeNPh)_2X$) toward the C−H bond insertion, cycloaddition, and dimerization reactions decreases with increasing atomic weight of the central atom X, i.e., in the order B > Al ≫ Ga > In > Tl. This trend agrees well with the singlet−triplet splitting of the group 13 carbenoid. Accordingly, based on the CM model,[16,17] our theoretical investigations suggest that the singlet−triplet splitting of a carbene analogue can be used as a diagnostic tool to predict its reactivity.

It is hoped that the present work can stimulate further research into this subject.

Acknowledgment. The authors are grateful to the National Center for High-Performance Computing of Taiwan for generous amounts of computing time. They also thank the National Science Council of Taiwan for financial support. Special thanks to the Reviewers for helpful suggestions and comments.

Supporting Information Available: This material is available free of charge via the Internet at http://pubs.acs.org.

OM060001L

(21) For recent reviews, see: (a) Grev, R. S. *Adv. Organomet. Chem.* **1991**, *33*, 125. (b) Esoudie, J.; Couret, C.; Ranaivonjatovo, H.; Satge, J. *Coord. Chem. Rev.* **1994**, *94*, 427. (c) Driess, M. *Coord. Chem. Rev.* **1995**, *145*, 1. (d) Mackay, K. M. In *The Chemistry of Organic Germanium, Tin, and Lead Compounds*; Patai, S., Ed.; Wiley: Chichester, U.K. 1995; Chapter 4. (e) Klinkhammer, K. W. *Angew. Chem., Int. Ed. Engl.* **1997**, *36*, 2320. (f) Barrau, J.; Rina, G. *Coord. Chem. Rev.* **1998**, *178*, 593. (g) Power, P. P. *J. Chem. Soc., Dalton Trans.* **1998**, 2939. (h) Tokitoh, N.; Matsumoto, T.; Okazaki, R. *Bull. Chem. Soc. Jpn.* **1999**, *72*, 1665. (i) Robinson, G. H. *Acc. Chem. Res.* **1999**, *32*, 773. (j) Power, P. P. *Chem. Rev.* **1999**, *99*, 3463. (k) Leigh, W. J. *Pure Appl. Chem.* **1999**, *71*, 453. (l) Tokitoh, N. *Pure Appl. Chem.* **1999**, *71*, 495. (m) Gruetzmacher, H.; Fassler, T. F. *Chem. Eur. J.* **2000**, *6*, 2317. (n) Kira, M.; Iwamoto, T. *J. Organomet. Chem.* **2000**, *610*, 236. (o) Tokitoh, N.; Okazaki, R. *Coord. Chem. Rev.* **2000**, *210*, 251. (p) Malcolm, N. O. J.; Gillespie, R. J.; Popelier, P. L. A. *J. Chem. Soc., Dalton Trans.* **2002**, 3333. (q) Tokitoh, N.; Okazaki, R. *The Chemistry of Organic Germanium, Tin and Lead Compounds*; Rappoport, Z., Ed.; Wiley: Chichester, 2002; Vol. 2, Chapter 13. (r) Klinkhammer, K. W. *The Chemistry of Organic Germanium, Tin and Lead Compounds*; Rappoport, Z., Ed.; Wiley: Chichester, 2000; Vol. 2, Chapter 42. (s) Lee, V. Y.; Sekiguchi, A. *Organometallics* **2004**, *23*, 2822. (t) Schleyer, P. v. R. *The Chemistry of Organic Silcon Compounds*; Rappoport, Z., Apeloig, Y., Eds.; John Wiley & Sons: London, 2001; pp 1−163, and reference therein.

(22) However, our B3LYP calculations indicate that the B═B dimer has the perpendicular structure **5**, while the other X═X dimers (X = Al, Ga, In, and Tl) have the trans-bent stucture **4**. The reason for this could be that the six-membered boron carbenoid species, $HC(CMeNPh)_2B$, has the triplet ground state.